Unusual Thermodynamic Properties and Nonergodicity in Ferroelectric Superlattices

Igor A. Kornev* and L. Bellaiche

Physics Department, University of Arkansas, Fayetteville, Arkansas 72701, USA

(Received 20 February 2003; published 12 September 2003)

The properties of $[Pb(Zr_{1-x_1}Ti_{x_1})O_3]_n/[Pb(Zr_{1-x_2}Ti_{x_2})O_3]_n$ superlattices, with a $2n$ period, are simulated using an *ab initio* based approach. The x_1 and x_2 compositions are chosen to be located across the morphotropic phase boundary of the corresponding disordered alloys, while the $(x_1 + x_2)/2$ average composition lies inside this boundary. These superlattices exhibit an unusual thermodynamic phase transition sequence, including a triclinic ground state. They also have the kind of peculiar free-energy landscape yielding nonergodicity. The effects responsible for these anomalies are discussed.

DOI: 10.1103/PhysRevLett.91.116103 PACS numbers: 68.65.Cd, 64.70.Kb, 77.80.Bh, 81.05.Zx

Ferroelectric heterostructures are of increasing technological interest because of their potential applications in advanced microsystems [1]. A particular type of heterostructure that has received recent attention is formed by superlattices, i.e., by compounds consisting of alternating layers made from different materials [2]. The properties of ferroelectric superlattices can be very different from those of their constituents, as a result of the complex nanostructure of these multilayer systems [3].

Another (currently unrelated) activity is taking place in ferroelectrics, namely, the investigation of the morphotropic phase boundary (MPB) of perovskite alloys [4]. This boundary was previously thought to discontinuously separate compositional regions of tetragonal and rhombohedral symmetry, for which the electrical polarization lies along a $\langle 001 \rangle$ and a $\langle 111 \rangle$ pseudocubic direction, respectively. The discovery of a monoclinic M_A phase in the MPB of $Pb(Zr_{1-x}Ti_x)O_3$ (PZT) solid solutions has drastically changed this picture [5]. [The notation for monoclinic phases is that of Ref. [6].] As a matter of fact, this M_A phase acts as a structural bridge between the tetragonal and rhombohedral phases, in the sense that the polarization in the M_A phase rotates between the pseudocubic $\langle 001 \rangle$ and $\langle 111 \rangle$ directions, as the Ti composition decreases within the MPB [7].

Independently of the two activities mentioned above, another research field is being intensively pursued. This field is the study of nonergodic systems, which are systems exhibiting properties that do not obey the usual Gibbs equilibrium statistical mechanics. Nonergodicity has been found in very diverse compounds, e.g., spin and structural glasses, granular systems, etc. [8]. Examples of observed behaviors associated with nonergodicity are an anomalous time dependency of macroscopic properties and/or a drastic dependency of such properties with thermal history [9]. The existence of various energetic minima that are separated by large barriers can drive a system to be nonergodic [10]. As a matter of fact, such a free-energy landscape can trap the system—for a long time at the experimental scale—in a particular valley, even if this valley is not the deepest one in energy. Consequently, the properties of such systems cannot be described by the Gibbs statistical averaging but rather require the use of new formalisms—e.g., the Edwards model—only involving the "blocked" configurations [10].

The aim of this Letter is twofold. First, we report that there is an unexplored class of ferroelectric superlattices that has unusual thermodynamic properties. This class is made by alternating layers of alloys having compositions lying just across their MPB. Second, we also predict that such layered systems can display nonergodicity.

More precisely, we theoretically investigate $[Pb(Zr_{1-x_1}Ti_{x_1})O_3]_n/[Pb(Zr_{1-x_2}Ti_{x_2})O_3]_n$ superlattices having (i) a $2n$ period, (ii) x_1 and x_2 compositions lying in the rhombohedral and tetragonal regions located just across the MPB of disordered PZT, and (iii) a $(x_1 + x_2)/2$ average composition yielding a monoclinic M_A phase in this MPB. These superlattices are chosen to be oriented along the [001] direction (see Fig. 1) and are denoted as $(n\text{PZT}x_1/n\text{PZT}x_2)$. Note that Ti and Zr atoms are randomly distributed within each (001) B plane under the constraint of fixed (x_1 or x_2) composition. We use

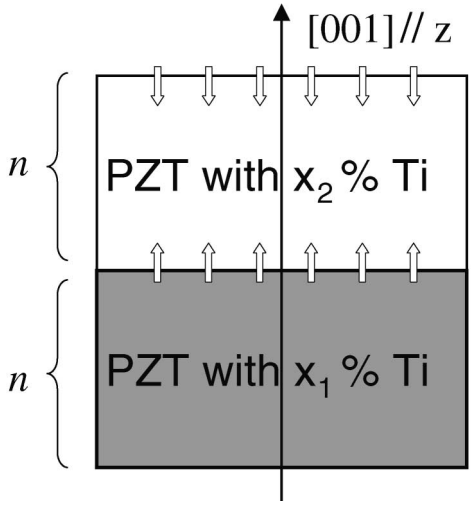

FIG. 1. Schematic illustration of the studied superlattices. n layers of PZT with a x_1 Ti concentration alternate with n layers of PZT with a x_2 Ti composition. The arrows indicate the strain field induced by the Ti and Zr size difference.

the first-principles-derived effective Hamiltonian to investigate finite-temperature properties of these superlattices. This approach has been successfully applied to different complex problems [11] and, in particular, has confirmed the presence of a M_A phase in the $T - x$ phase diagram of disordered $Pb(Zr_{1-x}Ti_x)O_3$ alloys [7]. The energy of this alloy effective Hamiltonian is given by [7]

$$\mathcal{H}(\{\mathbf{u}_i\},\{\mathbf{v}_i\},\eta_H,\{\sigma_j\}) = H_{\text{ave}}(\{\mathbf{u}_i\},\{\mathbf{v}_i\},\eta_H) + \sum_i [\Delta\alpha(\sigma_i)\mathbf{u}_i^4 + \Delta\gamma(\sigma_i)(u_{ix}^2u_{iy}^2 + u_{iy}^2u_{iz}^2 + u_{iz}^2u_{ix}^2)] + \sum_{ij}[R_{|j-i|}\mathbf{f}_{ji}\cdot\mathbf{v}_i + Q_{|j-i|}\mathbf{e}_{ji}\cdot\mathbf{u}_i]\sigma_j, \quad (1)$$

where the sum over i runs over all the unit cells, while the sum over j runs over the mixed sublattice sites. $\mathbf{u}_i$ is the (B-site-centered) local soft mode in unit cell i, $\{\mathbf{v}_i\}$ are the (A-site-centered) dimensionless local displacements that are related to the inhomogeneous strain inside each cell [12], η_H is the homogeneous strain tensor, and σ_j is defined to be $+1$ (respectively, -1) if site j is occupied by a Zr (respectively, Ti) atom. H_{ave} gathers five different kinds of energetic terms, for the PZT alloys, as mimicked by the so-called virtual crystal alloy approximation [7]: a local-mode self-energy, a long-range dipole-dipole interaction, a short-range interaction between soft modes, an elastic energy, and an interaction between the local modes and local strain [7,12]. $\mathbf{f}_{ji}$ (respectively, $\mathbf{e}_{ji}$) is a unit vector joining the B site j to the origin of $\mathbf{v}_i$ (respectively, $\mathbf{u}_i$). The $R_{|j-i|}$ and $Q_{|j-i|}$ parameters are related to alloying-induced intersite interactions, while $\Delta\alpha$ and $\Delta\gamma$ characterize the on-site contribution of alloying [7]. All the parameters entering Eq. (1) are derived from first-principles calculations. The total energy of the effective Hamiltonian is used in Monte Carlo (MC) simulations on large supercells—typically containing between 5000 and 40 000 atoms—mimicking the studied structures. 2×10^4 MC sweeps are first performed to equilibrate the system, and then 2×10^4 sweeps are used to get statistical averages. The outputs of the MC procedure are the local-mode vectors—whose supercell average is directly proportional to the macroscopic polarization—and the homogeneous strain tensor—which provides information about the crystallographic system.

Note that the x-, y-, and z axes are chosen along the pseudocubic [100], [010], and [001] directions, respectively. In other words, the z axis lies along the growth direction of the superlattices (see Fig. 1). Figure 2 shows the predicted x-, y-, and z-Cartesian coordinates (u_x, u_y, and u_z) of the local-mode vectors—averaged over all five-atom cells in our supercell—in (nPZT0.44/nPZT0.52), as a function of the temperature. Figures 2(a) and 2(b) correspond to a superlattice period associated with $n = 1$ and $n = 6$, respectively. The temperature is decreased in small steps in order to reach equilibrium. The PZT superlattice indexed by $n = 1$ exhibits a paraelectric state at high temperature, since u_x, u_y, and u_z are all null. This paraelectric state is tetragonal with a $4/mmm$ point group, rather than cubic, because of the atomic ordering existing along the [001] pseudocubic direction. As the temperature decreases, the (1PZT0.44/1PZT0.52) superlattice undergoes two phase transitions: the first transition occurs at $T \simeq 640$ K, resulting in a $2mm$ orthorhombic ferroelectric structure. This phase is characterized by a nonzero component of the polarization along a Cartesian axis that is perpendicular to the [001] direction (e.g., along the x axis). Then around $T \simeq 200$ K, there is a second transition towards another ferroelectric phase for which $u_x > u_y = u_z \neq 0$. This phase is triclinic [13]. To our knowledge, this is the first time that a triclinic ground state has been predicted to occur in the MPB area of any perovskite alloy, without applying an external electric field [14].

Interestingly, the temperature dependency of the local modes displayed in Fig. 2(a) is the same as in the

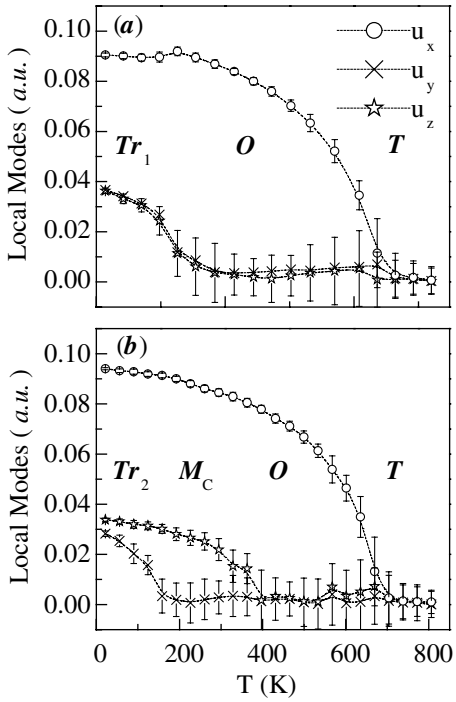

FIG. 2. (u_x, u_y, u_z) Cartesian coordinates of the local-mode vectors, averaged over all five-atom cells, as a function of temperature for (nPZT0.44/nPZT0.52) superlattices (as mimicked by $12 \times 12 \times 12$ supercells). (a) and (b) correspond to $n = 1$ and $n = 6$, respectively. The temperature has been rescaled as in Ref. [7]. T, O, and M_C refer to tetragonal, orthorhombic, and monoclinic phases, respectively. Tr_1 and Tr_2 are two different triclinic phases.

disordered PZT having the same overall composition of 48% [15]. However, unlike in the studied superlattices for which the z axis is different by symmetry from the other two axes because of the atomic ordering, the random PZT alloy does not have any distinct Cartesian direction. The phase transition sequence in the disordered alloy is thus paraelectric ($m\bar{3}m$) cubic → ferroelectric ($4mm$) tetragonal → ferroelectric (m) M_A monoclinic, rather than paraelectric ($4/mmm$) tetragonal → ferroelectric ($2mm$) orthorhombic → ferroelectric (1) triclinic as in the $n = 1$ superlattice.

Moreover, comparing Figs. 2(a) and 2(b) clearly demonstrates that increasing the periodicity of the superlattices drastically affects the phase transition sequence. In particular, one can notice that (6PZT0.44/6PZT0.52) differs from (1PZT0.44/1PZT0.52) by the existence of an additional structure thermally located in between the orthorhombic and triclinic phases. This additional phase is characterized by $u_x > u_y \neq 0$ and $u_z = 0$ and is thus of monoclinic M_C symmetry [16]. Another striking difference between the two superlattices concerns the triclinic state: increasing n from 1 to 6 leads to a splitting of the two smallest Cartesian components of the polarization; namely, it yields $u_x > u_y > u_z > 0$. The smallest component of the polarization in this triclinic ground state is thus along the ordering z direction, while, for symmetry reasons, the largest component of the polarization can be parallel (or antiparallel) to either the x axis—as found here—or the y axis. This results in a triclinic ground state that is 16-times degenerated.

Our calculations further predict that any studied (nPZTx_1/nPZTx_2) superlattice exhibits another minimum at low temperatures, in addition to the triclinic state. This minimum is a secondary minimum and is characterized by $u_z > u_x = u_y \neq 0$. The resulting phase is thus monoclinic M_A and is 8-times degenerated since the largest component of the polarization is along the ordering z axis. Figure 3 displays the 5 K internal energy—with respect to the paraelectric state—of both the global triclinic minimum and the secondary M_A minimum as a function of n for (nPZTx_1/nPZTx_2) superlattices with two different (x_1, x_2) combinations. These two minima are rather deep in energy (around $\simeq$ 84–86 meV/5 atoms) and are thus separated by large energetic barriers. This explains why we further find that the studied superlattices can be trapped in the secondary minimum (rather than desiring to go to the global minimum), when rapidly annealing the samples, or when applying and then removing an electric field (or a stress) along the [001] direction starting from the triclinic state. The existence of a multiwell and blocked-configuration free-energy landscape should drive nonergodicity in the (nPZTx_1/nPZTx_2) superlattices. We can imagine a nonergodic evolution for which the system will be distributed over the two different kinds of minima. Such a redistribution can increase the Edwards entropy [10] which characterizes

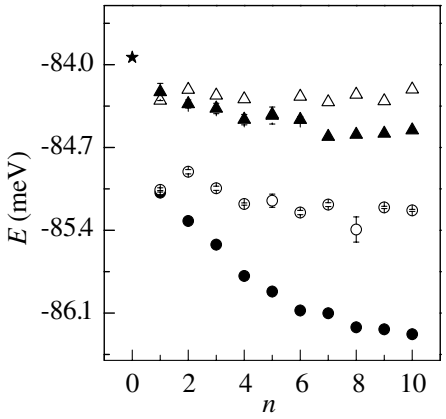

FIG. 3. Energy of the local M_A (white symbols) and global triclinic minima (black symbols) as a function of n in (nPZT0.44/nPZT0.52) (circles) and (nPZT0.46/nPZT0.50) (triangles) superlattices, at 5 K. The star denotes the total energy of the M_A ground state in disordered $PbZr_{0.52}Ti_{0.48}O_3$ alloys.

the disorder in the distribution of states of a nonergodic system over internal-energy minima. In this case, the evolution of the system is described by the time-dependent probability distribution over these minima. This dependency can be found by solving the Fokker-Planck equation, which is a very tedious task [17]. The predicted nonergodicity can be experimentally confirmed by looking at, for instance, nonmonotonic variations in the time evolution of x-ray diffraction patterns [18].

Figure 3 also reveals that the low-temperature monoclinic and triclinic phases are very close to each other in energy, typically less than 1 meV per five atoms, in any studied (nPZTx_1/nPZTx_2) system. This small energetic difference implies that several effects may change the symmetry of the ground state, that is, from triclinic to monoclinic M_A, or vice versa. Examples of such effects are compressive or tensile strain induced by a substrate, uniaxial or hydrostatic pressure, application of an electric field, and zero-point quantum vibrations.

We now look for the mechanisms responsible for the anomalous properties reported above. For that, we first take into account that the ground state of disordered PZT solid solutions with 48% Ti concentration is monoclinic M_A. It is thus characterized by $u_3 > u_2 = u_1 \neq 0$, with (u_3, u_2, u_1) being the largest, middle, and smallest Cartesian components of the local modes. This set of inequalities, if still satisfied in our studied layered systems, gives rise to two different structural phases in (nPZTx_1/nPZTx_2). One phase corresponds to the situation for which $u_3 = u_z$, that is, the largest component of the polarization is along the z axis. This solution is the secondary minimum of M_A symmetry that we found in (nPZTx_1/nPZTx_2). The second possibility corresponds to the case in which the largest component of the mode is along an axis perpendicular to the z direction, e.g., (u_3, u_2, u_1) = (u_x, u_y, u_z). This results in the triclinic

ground state of (nPZTx_1/nPZTx_2) with $n = 1$. This simple symmetry argument thus explains the existence of the two different minima. However, it is unable to explain why there is a splitting between the intermediate and smallest components of the polarization, and why this smallest component is along the ordering direction, for n larger than 1. To understand these effects, we performed different simulations, turning off and on the $R_{|j-i|}$ and $Q_{|j-i|}$ parameters of Eq. (1). We numerically found that the splitting between u_2 and u_1, and the fact that $u_1 = u_z$, is mainly caused by the $R_{|j-i|}$ parameter, which is related to the difference in ionic radius between Ti^{4+} (0.605 Å) and Zr^{4+} (0.72 Å) [19]. This size difference generates an inhomogeneous strain field that is oriented along the [001] direction in one of the interfaces while it is along the opposite $[00\bar{1}]$ direction at the other interface (see Fig. 1). These opposite strain fields, altogether with the coupling between local modes and strain, result in the reduction of the z component of the local mode with respect to its intermediate component u_2. This explains the characteristics of the triclinic phase—as well as the existence of the M_C phase for which $u_x > u_y \neq 0$ and $u_z = 0$, and occurring at higher temperature—depicted in Fig. 2(b).

In summary, we have used a first-principles-derived approach to study properties of short-period (nPZTx_1/nPZTx_2) superlattices, for which the x_1 and x_2 compositions are located across the MPB of disordered PZT while the $(x_1 + x_2)/2$ average composition lies inside this MPB. These superlattices exhibit a thermodynamic phase transition sequence that is different—by the number of phases as well as by the symmetry of these phases—from the corresponding sequence in the random PZT alloy having the same overall composition. In particular, the ground state of the superlattices is found to be triclinic. Moreover, (nPZTx_1/nPZTx_2) systems also have (deep) local minima of monoclinic M_A symmetry that are very close in energy from the global triclinic minima. This multivalley configuration can generate a nonergodic behavior. Furthermore, we revealed the mechanisms responsible for these unusual features. Finally, let us point out that the studied superlattices also exhibit interesting electromechanical responses. For instance, the existence of the triclinic ground state depicted in Fig. 2(b) leads to an enhancement of the χ_{33} dielectric susceptibility (≈ 1800 for $n = 10$) with respect to the disordered alloy having the same overall Ti composition (≈ 1500 for 48% of Ti).

This work is supported by ONR Grants No. N00014-01-1-0365 and No. N00014-01-1-0600 and NSF Grant DMR-9983678. We thank E. Salje for useful discussions.

*Also at Novgorod State University, Novgorod, Russia.

[1] R. Ramesh, S. Aggarwal, and O. Auciello, Mater. Sci. Eng. **32**, 191–236 (2001).

[2] T. Tsurumi, T. Suzuki, and M. Daimon, Jpn. J. Appl. Phys. **33**, 5192 (1992); M. Sepliarsky *et al.*, J. Appl. Phys. **91**, 3165 (2002).

[3] D. O'Neill, R. M. Bowman, and J. M. Gregg, Appl. Phys. Lett. **77**, 1520 (2000); Can Wang *et al.*, Appl. Phys. Lett. **82**, 2880 (2003).

[4] B. Noheda, Curr. Opin. Solid State Mater. Sci. **6**, 27 (2002); J.-M. Kiat *et al.*, Phys. Rev. B **65**, 064106 (2002).

[5] B. Noheda *et al.*, Appl. Phys. Lett. **74**, 2059 (1999).

[6] D. Vanderbilt and M. H. Cohen, Phys. Rev. B **63**, 094108 (2001).

[7] L. Bellaiche, A. Garcia, and D. Vanderbilt, Phys. Rev. Lett. **84**, 5427 (2000); Ferroelectrics **266**, 41–56 (2002).

[8] K. Binder and A. P. Young, Rev. Mod. Phys. **58**, 801 (1986).

[9] D. Viehland *et al.*, Phys. Rev. B **46**, 8013 (1992); M. T. Lacerda-Arôso *et al.*, J. Phys. Condens. Matter **13**, 2615 (2001).

[10] S. Edwards and P. W. Anderson, J. Phys. F **5**, 965 (1975); S. F. Edwards, in *Granular Matter: An Interdisciplinary Approach*, edited by A. Metha (Springer, New York, 1994).

[11] A. M. George, J. Íñiguez, and L. Bellaiche, Nature (London) **413**, 54 (2001); J. Íñiguez and L. Bellaiche, Phys. Rev. Lett. **87**, 095503 (2001); I. A. Kornev and L. Bellaiche, Phys. Rev. Lett. **89**, 115502 (2002).

[12] W. Zhong, D. Vanderbilt, and K. M. Rabe, Phys. Rev. B **52**, 6301 (1995).

[13] The different layers have the same transition temperatures as the superlattice as a whole, in the sense that the increases of the local modes averaged over the supercell (depicted in Fig. 2) are associated with simultaneous increases of the local modes inside each (001) layer.

[14] L. Bellaiche, A. Garcia, and D. Vanderbilt, Phys. Rev. B **64**, 060103 (2001).

[15] The $n = 1$ system is the superlattice that is the closest one to the disordered alloy since the latter can be thought of as the $n = 0$ superlattice. This explains why the $n = 1$ superlattice and the random alloy can exhibit similar macroscopic results. In particular, they both have a ground state characterized by a local mode having two equal Cartesian components that are smaller than the third component. The $n = 1$ superlattice chooses (for energetic reasons) to have this third component along the x axis, which thus results in $u_y = u_z$ (that is, a component of the local mode in the layer equal to another component perpendicular to the layer).

[16] The strain tensor associated with this solution is such as $\eta_1 \neq \eta_2 \neq \eta_3 \neq \eta_6 \neq 0$ and $\eta_4 = \eta_5 \equiv 0$. The resulting lattice vectors of the direct Bravais lattice are $\mathbf{a}_{M_C} = a_0[(1 + \eta_1), \frac{1}{2}\eta_6, 0]$, $\mathbf{b}_{M_C} = a_0[\frac{1}{2}\eta_6, 1 + \eta_2, 0]$, and $\mathbf{c}_{M_C} = a_0[0, 0, 1 + \eta_3]$, where $a_0 = 7.56$ Bohrs, which indicates that this solution is of monoclinic symmetry.

[17] H. Risken, *The Fokker-Planck Equation* (Springer, Berlin, 1989).

[18] V. M. Avdjukhina, A. A. Katsnelson, and G. P. Revkevich, Platinum Met. Rev. **46**, 169 (2002).

[19] R. D. Shannon, Acta Crystallogr. Sect. A **32**, 751 (1976).